Colloids and Surfaces B: Biointerfaces 72 (2009) 188–192

Contents lists available at ScienceDirect

Colloids and Surfaces B: Biointerfaces

journal homepage: www.elsevier.com/locate/colsurfb

# Amperometric glucose biosensor based on a gold nanorods/cellulose acetate composite film as immobilization matrix

Xiangling Ren, Dong Chen, Xianwei Meng, Fangqiong Tang*, Aiming Du, Lin Zhang

*Key Laboratory of Photochemical Conversion and Optoelectronic Materials, Laboratory of Controllable Preparation and Application of Nanomaterials, Technical Institute of Physics and Chemistry, Chinese Academy of Sciences, No. 2 Beiyitiao Zhongguancun, Beijing 100190, People's Republic of China*

ARTICLE INFO

*Article history:*
Received 5 January 2009
Received in revised form 13 March 2009
Accepted 1 April 2009
Available online 10 April 2009

*Keywords:*
Gold nanorods
Immobilization enzyme
Glucose oxidase
Biosensor

ABSTRACT

We report on the utilization of gold nanorods to create a highly responsive glucose biosensor. The feasibility of an amperometric glucose biosensor based on immobilization of glucose oxidase (GOx) in gold nanorod is investigated. GOx is simply mixed with gold nanorods and cross-linked with a cellulose acetate (CA) medium by glutaraldehyde. The adsorption of GOx on the gold nanorods is confirmed by X-ray photoelectron spectroscopy (XPS) measurements. Circular dichroism (CD) and UV-spectrum results show that the activity of GOx was preserved after conjugating with gold nanorods. The current response of modified electrode is 10 times higher than that of without gold nanorods. Under optimal conditions, the biosensor shows high sensitivity ($8.4\,\mu A\,cm^{-2}\,mM^{-1}$), low detection limit ($2 \times 10^{-5}$ M), good storage stability and high affinity to glucose ($K_m^{app} = 3.84$ mM). A linear calibration plot is obtained in the wide concentration range from $3 \times 10^{-5}$ to $2.2 \times 10^{-3}$ M.



## 1. Introduction

Glucose biosensors would provide the possibility of carrying out analytical and diagnostic procedures simply and rapidly. They allow greater ease of use with opportunities for self-monitoring by some special groups such as diabetics. With improved glucose control it is possible that some of the long-term diabetic syndromes, such as retinal and kidney damage, would be avoided.

The measurement principle of glucose biosensor relies upon the immobilization of glucose oxidase (GOx) on the surface of various electrodes and the detection of the current associated with the redox of GOx to glucose. GOx is a flavin enzyme with flavin adenine dinucleotide (FAD) as the redox prosthetic group, and its biological function is to catalyze glucose to gluconolactone. The performance of an enzyme electrode often depends on the method of enzyme immobilization when fabricating biosensors [1]. Therefore, the technique used to immobilize the enzyme is one of the crucial factors in developing a reliable biosensor, and new immobilized schemes and advanced materials that can improve the analytical capacities of sensor devices are highly desired.

Over the last decade, nanostructured materials attracted interest of many researchers due to their unique physical and chemical properties [2]. Catalysis is one of the most frequently used characters of nanomaterials. Besides that, they also facilitate electron transfer [3] and can be easily modified using a wide range of biomolecules and chemical ligands. Many kinds of nanometer materials such as Au [4,5], Ag [6], Pt [7], $SiO_2$ [8] and their compound [9] have been used to immobilize enzymes and to construct biosensors. However, the majority of the nanomaterials modified biosensors reported previously were based on the zero-dimensional (0D) nanoclusters.

Following the improvement of nanoscience and nanotechnology, the challenge in application of nanomaterials is to control not only the particle sizes but also the particle shapes and morphologies. Shape control is an alternative tool for adjusting the optical, electronic or catalytic properties of nanomaterials [10]. Such as, the one-dimensional (1D) nanostructures have been the key structural blocks in the new generation of electronics, sensors, and photonics materials. Carbon nanotube has been used to immobilize biological molecules in order to fabricate biosensors [11,12]. Recently, Jin and co-workers reported a uric acid biosensor based on the ZnO nanorods [13]. To the best of our knowledge, there are fewer reports on using the gold nanorods to fabricate the glucose biosensor.

In this paper, gold nanorods are introduced to the research of the glucose biosensors. We use gold nanorods because gold nanomaterials are biocompatible and they are one of the most important nanomaterials which were used to fabricate biosensors. Some measurements have been used to investigate the surface interaction between GOx and gold nanorods. X-ray photoelectron spectroscopy (XPS) measurements provide evidence of enzyme adsorption onto gold nanorods. Circular dichroism (CD) and UV-spectrum results show that the activity of GOx is preserved after conjugating with gold nanorods. Amperometric measurements results show that the gold nanorod can significantly enhance the current sensitivity of

* Corresponding author. Tel.: +86 10 82543521; fax: +86 10 62554670.
*E-mail address:* tangfq@mail.ipc.ac.cn (F. Tang).

0927-7765/$ – see front matter © 2009 Elsevier B.V. All rights reserved.
doi:10.1016/j.colsurfb.2009.04.003

GOx enzyme electrodes. The performance of the obtained electrodes with respect to linear range, reproducibility, response time, and stability is presented and discussed.

## 2. Experimental

### 2.1. Chemicals and reagents

GOx was extracted from *Aspergillus niger* (Sigma company, 118 U/mg). β-D-glucose and cetyltrimethylammonium bromide (CTAB) were purchased from Sigma. L(+)-ascorbic acid (99%), silver nitrate ($AgNO_3$), chlorauric acid ($HAuCl_4{\cdot}3H_2O$), sodium borohydride ($NaBH_4$) and cellulose acetate (CA) were products of Beijing Shiji Company. All the chemicals were used without further purification. All solutions were prepared with deionized water.

### 2.2. Preparation of gold nanorods

Gold nanorods were prepared by a seed-mediated growth approach reported by Murphy and co-workers [14,15].

#### 2.2.1. Preparation of gold seed

A 8 mL aqueous solution containing $9 \times 10^{-2}$ M CTAB and $3 \times 10^{-4}$ M $HAuCl_4$ was prepared in a conical flask. Next 0.5 mL of ice cold 0.1 M $NaBH_4$ solution was added to the solution while stirring. The solution turned brownish yellow immediately after adding $NaBH_4$, indicating particle formation.

#### 2.2.2. Preparation of gold nanorod

$AgNO_3$ (0.15 mL, $4 \times 10^{-3}$ M) was added to 10 ml of $9.5 \times 10^{-2}$ M CTAB solution. To this solution, 0.1 mL of $4.2 \times 10^{-2}$ M $HAuCl_4$ was added, and after gentle mixing of the solution 0.06 mL of 0.1 M ascorbic acid was added. The final step was the addition of 0.01 mL of the seed solution to the growth solution. The temperature of the growth medium was kept constant at 25 °C in all the experiments. Then the precipitate was centrifugated, washed with deionized water and diluted to 5 mL with deionized water.

### 2.3. Preparation of enzyme electrodes

The platinum electrode with a diameter of 1 mm was boiled in nitric acid for 5 min and washed in redistilled water. The aqueous solution of GOx (10 μL, 1 U/μL) was added to 10 μL gold nanorods solution to form mixture and then dried on the Pt electrode. A 20 μL of glutaraldehyde was applied on the resulting electrode to cross-link the enzyme. 400 μL gold nanorods were added to 2 mL CA solution (2%) in acetone in a 5 mL beaker. And then the platinum electrode was dipped into the mixture for 5 min and dried in air. These electrodes were stored at 4 °C for 24 h before measurement.

The enzyme electrode without gold nanorods used as comparison was prepared by the same method as described above except added gold nanorods.

### 2.4. Apparatus and measurements

Transmission electron microscope (TEM) of gold nanorods was obtained with a JEOL-200CX electron microscope, operating at 160 kV. V-570 UV/VIS/NIR spectrophotometer (Jasco, Japan) was used to measure the UV-spectrum of the samples.

XPS was performed on gold nanorods, GOx, and GOx–Au. GOx–Au was prepared by first dissolving GOx in a solution of gold nanorods and incubating for 24 h at 4 °C. The solution was then centrifuged at 12,000 rpm for 10 min, and the supernatant was removed. Deionized water was then added, and the gold nanorods were resuspended by vortexing. This washing procedure was repeated at least three times to remove any unbound GOx. The samples of gold nanorods, GOx, and GOx–Au were dispensed onto the quartz substrate and dried at room-temperature overnight. XPS measurements were recorded with a PHI Quantera SXM system with monochromatic Al Kα X-rays (photon energy of 280.0 eV). The background pressure was about $6.7 \times 10^{-8}$ Pa. The binding energies were referenced to the C1 s line at 284.8 eV from adventitious carbon.

The CD spectra were taken using a Jasco J-810 spectropolarimeter. Quartz cells of 1 mm optical path length were used for all CD measurements of GOx (GOx concentration = $6.5 \times 10^{-7}$ M) and GOx–Au (GOx:Au = 1:1 molar ratio) solutions. The phosphate buffer ($Na_2HPO_4$–$NaH_2PO_4$, pH 6.8) was used to prepare these solutions. The spectra were analyzed for the content of secondary structure by using the software accompanying the spectropolarimeter.

Cyclic voltammetry studies used a CHI604B electrochemical workstation (Shanghai Chenhua Apparatus Corporation, China). All experiments were carried out using a three-electrode cells equipped with a Pt-wire as counter electrode and an Ag/AgCl electrode as reference electrode. The applied scan rate was 50 mV/s.

Amperometric measurements were carried out using a three-electrode cell consisting of an enzyme working electrode, a counter electrode of platinum wire, and a reference electrode of Ag/AgCl. Measurements were conducted in a 5 ml phosphate buffer ($KHPO_4$–NaOH, pH 6.8) cell at 35 °C. A fixed potential of 0.4 V was applied to this electronic cell. Firstly, working electrode and reference electrode were put into a phosphate solution at 35 °C. When background current reached a constant value, different concentrations (from 0.2 to 5.5 mM) of β-D-glucose solution were added. Then response current was noted down, and background current was deducted, and the correlation between response currents and different concentrations of glucose solution was obtained.

## 3. Results and discussion

### 3.1. Characterization of biocomposite of GOx–gold nanorods

Fig. 1A shows the typical nanostructures of Au nanorods synthesized by the method described above. In this sample, the average diameter of nanorods is 16 nm and the average length is 40 nm.

XPS measurements of the GOx, gold nanorods, and GOx–Au samples were performed to confirm whether the GOx was adsorbed onto the gold nanorods during the incubation step [16]. Fig. 1B(a) shows the XPS spectra for GOx and shows a predominant presence of carbon (62%), oxygen (25%), and nitrogen (14%) via the detection of the C1 s, O1 s, and N1 s peaks. We think these nitrogen atoms are present in the amide bonds in the enzyme's polypeptide chain. The spectra of gold nanorods show an Au4f peak for gold (10%). However, nitrogen (N1 s peak) is undetected. In contrast, Fig. 1B(c) shows the spectra of GOx–Au. Once again, the distinct N1 s peak for nitrogen (7%) is shown. These results provide evidence that enzyme molecules were adsorbed onto the gold nanorods.

Recently, CD has been widely used to analyze the main properties and features of enzyme solutions and films [17]. The most utilized form of CD spectroscopy is far-UV CD (190–250 nm), which is analyzed to estimate the secondary structure content of the proteins due to correspond to electronic transitions of the backbone chromophore of the enzyme [18]. In the present work, CD spectra are used to characterize the secondary structure of GOx after bioconjugating with gold nanorods. Fig. 1C displays the CD spectra of GOx and GOx–Au bioconjugates. Spectral analysis can provide estimates of the secondary structure content, and the results of such analysis are presented in Table 1. Indeed, it can be seen that the CD spectrum of GOx–Au bioconjugates looks similar to the pure GOx, but the peak has slightly less intensity. It indicated that the GOx have been adsorbed on the surface of gold nanorods. In fact, the similar secondary structure content of GOx and GOx–Au indicated that

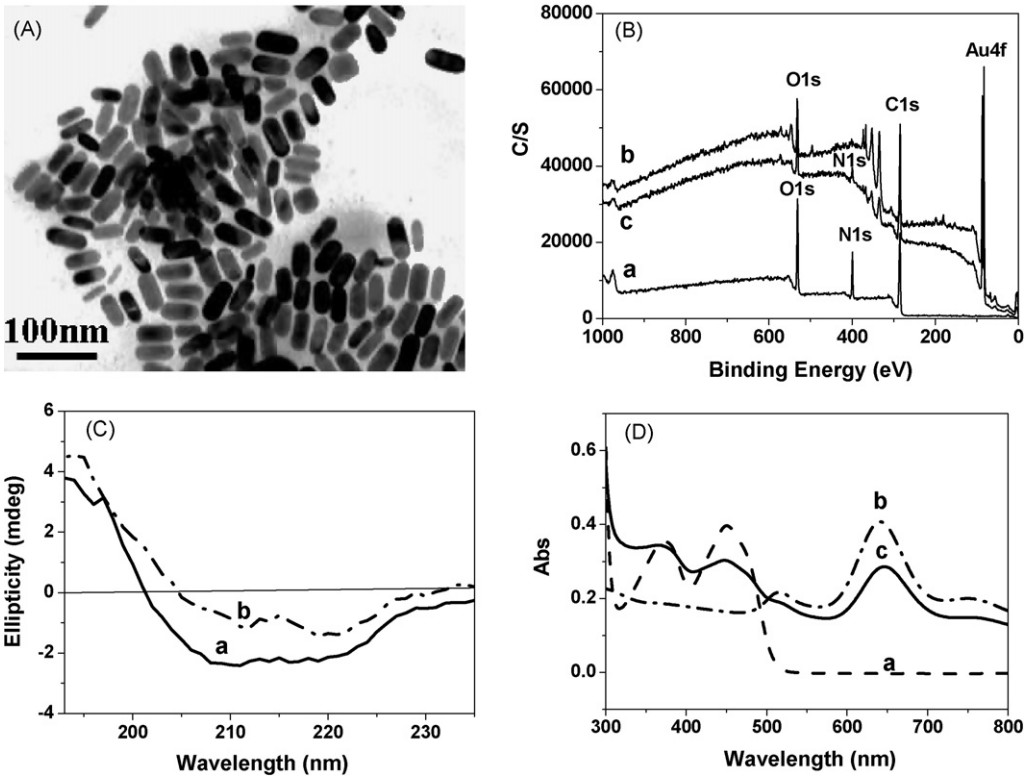


**Fig. 1.** (A) Typical TEM image of the gold nanorods; (B) survey X-ray photoelectron spectra for (a) GOx, (b) gold nanorods, and (c) GOx–Au; (C) CD spectra of pure GOx (a) and GOx–Au bioconjugates (b); (D) UV–vis spectra of (a) GOx, (b) gold nanorods, and (c) GOx–Au bioconjugate.

the secondary structure of GOx was preserved after conjugating with gold nanorods [19].

Fig. 1D shows the absorption spectrums of GOx, gold nanorods and GOx–gold nanorods. Pure GOx had absorption peak in the visible region with maximum values at 374 nm and 450 nm (curve a), which were consistent with previous report [20]. For the gold nanorods, the surface plasmon absorption of them had two bands: a strong long-wavelength band around 641 nm due to the longitudinal oscillation of electrons and a weak short-wavelength band around 516 nm due to the transverse electronic oscillation (curve b). After bioconjugation of GOx with Au (curve c), these absorption bands had slightly shifted to 364, 447 and 646 nm. Considering the result of the CD spectrum, the shifts of the absorbance maximum of GOx may attribute to the interaction between gold nanorods and GOx, which also indicates that GOx have been adsorbed on the surface of gold nanorods.

### 3.2. Cyclic voltammetric characterization

Cyclic voltammetry of an electroactive species such as ferricyanide is a valuable tool for testing the kinetic barrier of the interface. The electron transfer between a solution species and the electrode must occur by tunneling either through the barrier or through the defects in the barrier [21,22]. Therefore, it is chosen as a marker to investigate the changes of electrode behavior [23]. Fig. 2 shows cyclic voltammograms (CVs) of differently modified electrodes in 5.0 mM ferricyanide solution. For the bare Pt electrodes, the well-defined oxidation and reduction peaks caused by the $Fe^{3+}/Fe^{2+}$ redox couples were noticed in forward and reverse scan (curve a). After the electrode modified by CA, an obvious decrease in reduction and oxidation peaks was observed (curve b). This may be due to the insulation properties of the CA membrane, which can block the electron transfer between the solution and the base Pt electrode. When gold nanorods were embedded in the CA membrane, the current response of CVs could be increased, indicating the enhancing effect of the gold nanorods on the electric conductivity of the enzyme electrode. This might be because gold nanorods have great effects on the permeability of CA film, which could provide a conductive path through the composite immobilization membrane matrix.

**Table 1**
Enzyme conformation of pure GOx and GOx–Au bioconjugates.

| | α-Helix (%) | β-Sheet (%) | $\alpha/\beta$ |
|---|---|---|---|
| GOx | 14 | 38 | 0.37 |
| GOx–Au | 10 | 42 | 0.24 |

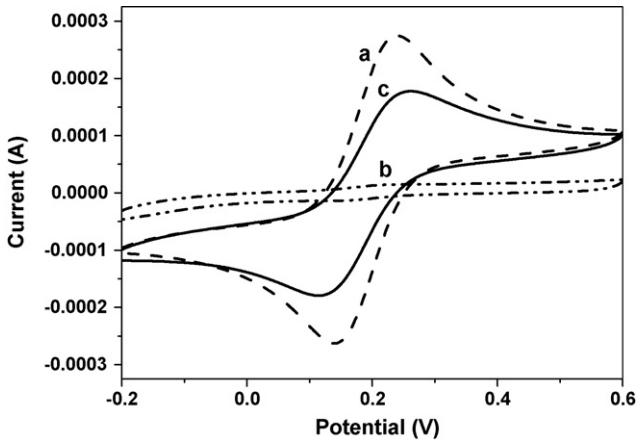


**Fig. 2.** Cyclic voltammograms of different modified electrodes: (a) bare Pt, (b) CA/Pt, and (c) CA/Au nanorods/GOx/Pt. Supporting electrolyte, 5 mM $Fe(CN)_6^{3-}$ + 0.1 M KCl; scan rate, 50 mV $s^{-1}$.

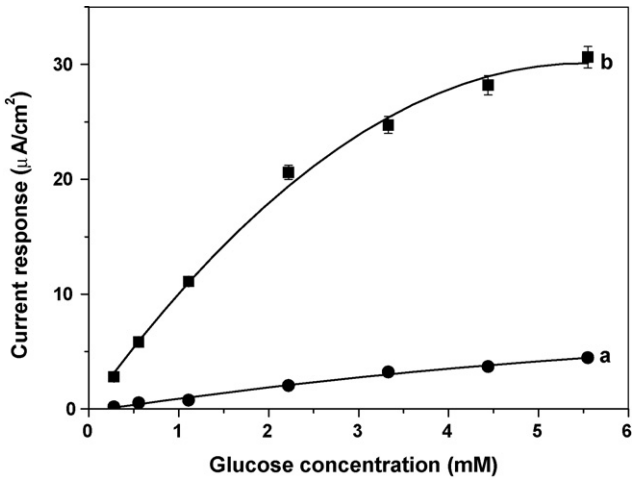


**Fig. 3.** Effect of gold nanorods on the GOx enzyme electrode current response (a) without nanorods; (b) with gold nanorods. The applied potential is 0.4 V vs. Ag/AgCl and the temperature is 35 °C.

### 3.3. The current response curves of the immobilized GOx electrode with gold nanorods

Fig. 3 represents the comparation of the current response between GOx electrodes with and without gold nanorods. This result indicates that Au nanorods can dramatically enhance the current response of the electrode. For example, when glucose concentration is 2.2 mM, the current density of the electrode without nanorods is 2 μA $cm^{-2}$, and that of the electrode with gold nanorods is 20 μA $cm^{-2}$. The steady-state response time for the electrode containing Au nanorods is less than 20 s. These results proved that gold nanorods can play an important role in adsorption of enzyme due to their large specific surface area. Many reports [24,25] have given some evidence that the surface of nanomaterials would facilitate the immobilization of enzyme, and improve the activity and stability of the enzyme. In this system, gold nanorods could adsorb large amount of GOx molecules and then increase the response of the enzyme electrode. On the other hand, from cyclic voltammograms we know Au nanorods can improve the conductivity of the enzyme electrode. So the Au nanorods function as conducting wires between the enzyme and the electrode surface, and facilitate electron transfer between them, then the capability of the GOx electrode can be improved.

### 3.4. Effect of applied potential and temperature on the glucose biosensor

The effect of applied potential on the biosensor response was studied (shown in Fig. 4A). The applied potential was evaluated at 2.2 mM glucose over the potential range from 0.2 to 0.8 V. When the applied potential increased from 0.2 to 0.6 V, the response current of the biosensor would accordingly increase. However, the current would decline when the applied potential exceeds 0.6 V. At the same time, when the applied potential exceeds 0.4 V, the background current of the biosensor would also increase and reach a rather high value. To avoid interference at high applied potential, a potential of 0.4 V is selected as the applied potential for amperometric measurement.

Fig. 4B shows the effect of the temperature on GOx–gold nanorod biosensor. In 2.2 mM glucose solution, the temperature stepped increases from 0 to 70 °C. To our surprise, the current response of biosensor increases with temperature increasing from 0 to 60 °C,

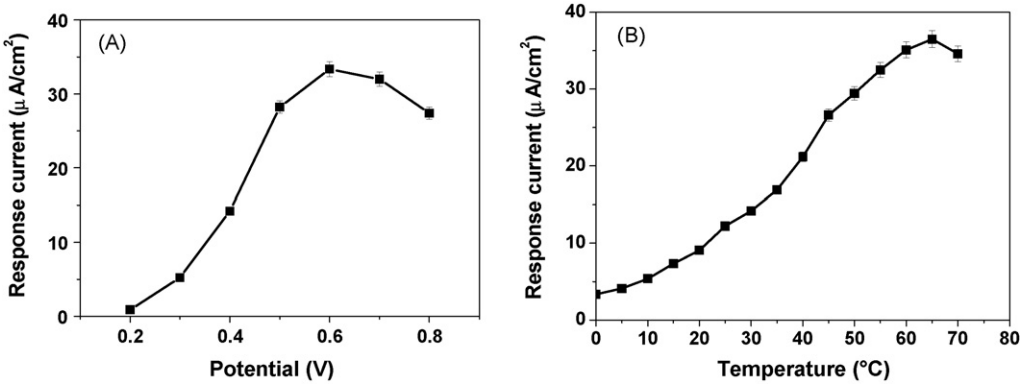


**Fig. 4.** (A) Effect of applied potential on the response of the biosensor to 2.2 mM glucose; (B) effect of temperature on the response of biosensor to 2.2 mM glucose.

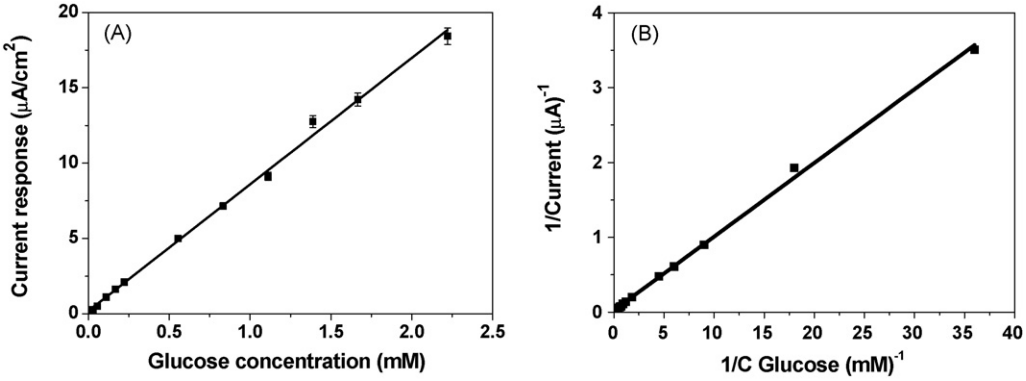


**Fig. 5.** (A) The calibration curve of the biosensor under the optimized conditions; (B) the illustrates the Kinetic analysis of electrocatalytic anodic currents at different glucose concentration according to Lineweave–Burk equation.

and then slightly declines. This result indicates that the enzyme bioconjugated with gold nanorods has good thermodynamic stability, which could benefit the preservation of enzyme electrode. To simulate the temperature of human body, temperature of 35 °C is selected for this work.

### 3.5. Calibration of the enzyme electrode

Fig. 5A displays the calibration curve of the biosensor. The linear range scans the concentration of glucose from $3 \times 10^{-5}$ to $2.2 \times 10^{-3}$ M with a correlation coefficient of 0.9985 and a sensitivity of 8.4 μA cm$^{-2}$ mM$^{-1}$ is obtained, which is much higher than those of 2.43 μA cm$^{-2}$ mM$^{-1}$ for GOx immobilized in boron-doped carbon nanotubes [26] and 6.5 μA cm$^{-2}$ mM$^{-1}$ based on GOx/colloidal gold nanoparticles immobilizing in nafion film [27]. The detection limit is $2 \times 10^{-5}$ M at a signal-to-noise ratio of 3.

The apparent Michaelis–Menten constant ($K_m^{app}$), a reflection of the enzymatic affinity, is calculated to be 3.84 mM according to the Lineweaver–Burk equation (determined from the slope of the linear part of the calibration, in Fig. 5B). The $K_m^{app}$ value is lower than 27 mM for native GOx in solution [28], 20 mM for GOx bound to self-assembled monolayer electrode [29], 10.5 mM for GOx entrapped in chitosan/gold nanoparticles multiplayer films [30], 9.3 mM for GOx immobilized in single-walled carbon nanotubes hybrid matrix [16], 6.34 mM for GOx in titania sol–gel membrane [31], indicating that the present electrode exhibits higher affinity to glucose of the GOx in the biocomposite.

### 3.6. Reproducibility and storage stability of the enzyme electrode

The reproducibility of response current of the GOx enzyme electrode was investigated at a glucose concentration of 2.2 mM. The relative standard deviation (RSD) of the biosensor was 2.3% for 10 successive measurements. The RSD for five biosensors were prepared at same conditions was 7.2%.

The stability of the enzyme electrode was also investigated by amperometric measurements in the presence of glucose with 2.2 mM over a month period. The current response of biosensor retained about 80% of its original response after storing.

## 4. Conclusions

This study develops a novel method to fabricate the glucose biosensor based on immobilization of GOx on Au nanorods. The XPS measurements provide evidence of enzyme adsorption onto gold nanorods. The CD and UV-spectrum results show that the activity of GOx can be maintained after bioconjugation with Au nanorods. The experimental results indicate the enzyme electrode containing Au nanorods significantly enhances the response current compared with the electrode containing no nanorods. This is due to the strong adsorption property of Au nanorods and the good electrical conducting property of Au. The cyclic voltammograms prove that the Au nanorods can improve the conductivity of the enzyme electrode. The biosensor also exhibits high sensitivity, low detection limit, wide linear range, good storage stability and reproducibility, and high affinity to glucose of the GOx in the biocomposite. This composite film can easily extend to immobilize other biomolecules.

## Acknowledgements

Support for this research by grants from the National Natural Science Foundation of China (project nos. 60602006, 60736001) and the Knowledge Innovation Program of the Chinese Academy of Sciences (TYF0808) is gratefully acknowledged.

## References

[1] Y.C. Liu, T.Y. Yu, Polym. Rev. 37 (1997) 459.
[2] S. Hrapovic, Y. Lui, K.B. Male, J.H.T. Luong, Anal. Chem. 76 (2004) 1083.
[3] J. Wang, M. Musameh, Anal. Chem. 75 (2003) 2075.
[4] Q. Xu, C. Mao, N.N. Liu, J.J. Zhu, J. Sheng, Biosens. Bioelectron. 22 (2006) 768.
[5] Y. Xiao, F. Patolsky, E. Katz, J.F. Hainfeld, I. Willner, Science 299 (2003) 1877.
[6] X.L. Ren, X.W. Meng, D. Chen, F.Q. Tang, J. Jiao, Biosens. Bioelectron. 21 (2005) 433.
[7] J.S. Ye, A. Ottova, H.T. Tien, F.S. Sheu, Bioelectrochemistry 59 (2003) 65.
[8] H.P. Yang, Y.F. Zhu, Talanta 68 (2005) 569.
[9] X.L. Ren, X.W. Meng, F.Q. Tang, Sens. Actuators B 110 (2005) 358.
[10] Z.L. Wang, J.H. Song, Science 312 (2006) 242.
[11] Y.H. Lin, F. Lu, Y. Tu, Z.F. Ren, Nano Lett. 4 (2004) 191.
[12] D. Wen, Y. Liu, G.C. Yang, S.J. Dong, Electrochim. Acta 52 (2007) 5312.
[13] F.F. Zhang, X.L. Wang, S.Y. Ai, Z.D. Sun, Q. Wan, Z.Q. Zhu, Y.Z. Xian, L.T. Jin, K. Yamamoto, Anal. Chim. Acta 519 (2004) 155.
[14] L. Gou, C.J. Murphy, Chem. Mater. 17 (2005) 3668.
[15] T.K. Sau, C.J. Murphy, Langmuir 20 (2004) 6414.
[16] Y.D. Wang, P.P. Joshi, K.L. Hobbs, M.B. Johnson, D.W. Schmidtke, Langmuir 22 (2006) 9776.
[17] M. Shimizu, K. Kobayashi, H. Morii, K. Mitsui, W. Knoll, T. Nagamune, Biochem. Biophys. Res. Commun. 310 (2003) 606.
[18] J.N. Herron, W. Jiskoot, D.J.A. Crommelin, Physical Methods to Characterize Pharmaceutical Proteins, Plenum Press, New York, 1995.
[19] G.L. Dai, J.R. Li, L. Jiang, Colloids Surf. B 24 (2002) 171.
[20] Q.J. Chi, J.D. Zhang, S.J. Dong, E.K. Wang, J. Chem. Soc., Faraday Trans. 90 (1994) 2057.
[21] S. Bharathi, M. Nogami, S. Ikeda, Langmuir 17 (2001) 1.
[22] J. Jia, B. Wang, A. Wu, G. Cheng, Z. Li, S. Dong, Anal. Chem. 74 (2002) 2217.
[23] D.P. Tang, R. Yuan, Y.Q. Chai, X. Zhong, Y. Liu, J.Y. Dai, L.Y. Zhang, Anal. Biochem. 333 (2004) 345.
[24] Z.J. Chen, X.M. Ou, F.Q. Tang, L. Jiang, Colloids Surf. B 7 (1996) 173.
[25] E. Katz, I. Willner, J. Wang, Electroanalysis 16 (2004) 19.
[26] X.L. Chen, J.H. Chen, C.Y. Deng, C.H. Xiao, Y.M. Yang, Z. Nie, S.Z. Yao, Talanta 76 (2008) 763.
[27] S. Zhao, K. Zhang, Y. Bai, W.W. Yang, C.Q. Sun, Bioelectrochemistry 69 (2006) 158.
[28] M.J. Rogers, K.G. Brandt, Biochemistry 10 (1971) 4624.
[29] A.S.N. Murthy, J. Sharma, Anal. Chim. Acta 363 (1998) 215.
[30] B.Y. Wu, S.H. Hou, F. Yin, J. Li, Z.X. Zhao, J.D. Huang, Q. Chen, Biosens. Bioelectron. 22 (2007) 838.
[31] J.H. Yu, S.Q. Liu, H.X. Ju, Biosens. Bioelectron. 19 (2003) 401.